LOW REYNOLDS NUMBER SWIMMING IN TWO DIMENSIONS

ALEXANDRE CHERMAN
Fundação Planetário
Av. Pe. Leonel Franca, 240, Rio de Janeiro, Brazil, 22451-000

JOAQUíN DELGADO
Departamento de Matemáticas, Universidad Autónoma Metropolitana-Iztapalapa
Av. Michoacán y la Purísima, 09340, Mexico

FERNANDO DUDA
Departamento de Mecânica da UFRJ
Cidade Universitária, Rio de Janeiro, 21944-970, Brazil

KURT EHLERS
California State University, Monterey Bay
100 Campus Center, Seaside CA, 93955-8001, USA

JAIR KOILLER
Visiting Position. Instituto de Matemática da Universidade Federal Fluminense
Av. Mario Santos Braga, s/n Niteroi, 24020-140 Brasil

RICHARD MONTGOMERY
University of California, Santa Cruz
CA, 95064, USA

A geometrical approach for low Reynolds number swimming was introduced by Shapere and Wilczek[1]. Here we pursue some developments for the two dimensional theory. The outer membrane or the ciliary envelope of the planar organism is represented by the conformal image of the unit circle. Power expenditures and velocities can be computed using complex variable techniques. As an example, we present the calculations for a self deforming ellipse. The results compare well with observations for the nematode *Turbatrix aceti*. We also compute the most efficient swimming stroke, using the criterion efficiency = velocity/hydrodynamical power. A pattern noticed by SW for the circle and the sphere is confirmed: efficiency is optimized around certain high order geometric modes. For the case of a deforming membrane, these modes require great mechanical stress. However, such high order geometric modes are easily emulated by ciliary envelopes without extra (mechanical) power expenditure. Therefore, coordinated spatio-temporal *ciliary* movements, besides providing an inherent maneuverability, have the added advantage of saving energy.

1 Introduction

We have been interested in nonholonomic motion and in microswimming since two of us (JK and RM) listened an inspiring talk by Frank Wilczek at Cornell, about ten years ago. Our general program was presented in [3] and in particular, we described the collective "N-body probem" of microswimming. Here N can be very large! (We hope this catchword to be somewhat related to Celestial Mechanics.)

Microscopic organisms propel themselves in an inertialess environment. Shapere and Wilczek[1,2], 1989, henceforth SW, showed that the rotation and translation of a swimming circular organism can be described by the *holonomy* of a connection on a principal bundle (whose structure group is the group of Euclidean motions). Actually at this point the mathematical structure is only formal: The base space is infinite dimensional and consists of all possible shapes of the microorganism (*the shape space*) and could be modelled by a convenient functional space of embedings.

If the amplitude of the swimming motions consist of small amplitude surface oscillations (i.e a *stroke*), then the holonomy can be computed using the curvature elements of this connection, computed at the average shape, the base shape.

We report here our findings in the two dimensional context, the first results appearing in[4]. There are very powerful techniques for solving the Stokes equations in the plane and it is possible to compute the Stokes curvature (the covariant derivative of the Stokes connection) for any base shape that is the conformal image of the circle. We present some corrections to SW (concerning only the rotational part of the connection). We also compute the power expenditure operator, details appearing in[5].

We discuss the case of an elliptical swimmer. Two of the major modes of swimming can be studied with this model: that of an organism with a self deforming outer membrane, and that of a slender organism that uses undulatory body motions. The results for the slender body using undulatory cycles provide a good model for the nematode *Turbatrix aceti*.

We numerically compute the most efficient axially symmetric swimming (the efficiency notion here is simply that efficiency = velocity/power). We verify that they are governed by certain high order geometric modes, following the same pattern as SW found for the circle and the sphere. Comparisons between different efficiency concepts are given in [15].

It is most important to notice that for a *deforming membrane*, high order geometric modes require great mechanical stress. On the other hand, such high order geometric modes are easily emulated by *ciliary envelopes*,

without extra mechanical power expenditure! Coordinated spatio-temporal ciliary movements, besides providing an inherent maneuverability, have the further advantage of saving energy[a].

In an article to be submited elsewhere[6], the curvatures for the three dimensional case of an ellipsoidal organism are presented, extending the results of Lighthill[8] , Blake[9] , and Shapere and Wilczek[2] . With little extra work, one can also make a direct comparison of a sphere with an infinite swimming sheet for the swimming velocity, power output, and optimal combination of tangential to normal components of the surface distortions.

2 The planar swimmer

The fluid domain is represented by the complex z-plane. A fluid velocity field will be given by the real and imaginary parts of complex valued functions $v: \mathbb{C} \to \mathbb{C}$. The outer membrane or the ciliary envelope C of the planar swimmer will be represented by the unit circle $\gamma = \{\xi \in \mathbb{C} \mid \ |\xi| = 1\}$ under the conformal map

$$z = \omega(\xi) = R(\xi + \frac{m_1}{\xi} + \cdots + \frac{m_n}{\xi^n}), \tag{1}$$

where R is a real number. While the organism's physical shape is represented by a closed curve in the z-plane, we will make our computation of the curvature in the ξ-plane where the organisms shape is parametrized by the unit circle.

As a basis (*modes*) for the vector fields on C we will choose the *push forward under composition* (not using the jacobian matrix), of the basis of Fourier modes on the unit circle: $V = \sigma^{n+1}$, where $\sigma = e^{i\theta}$. We call this the *hodographed Fourier basis*, or for short, the Fourier basis. The order of the modes is then tagged by index[b] n.

We will supress the vector notation thus $V(\sigma)$ is a complex valued function on C representing the boundary vector field $\vec{V}$, and $v(z, \bar{z})$ is a complex valued function on the exterior of C representing the fluid velocity field $\vec{v}$ with $\vec{v}_{|C} = \vec{V}$.

2.1 Stokes Equations in the plane

For the planar problem there is a very powerful technique, developed by Mkhelishvili[11] in the context of planar elasticity theory, that uses Cauchy integrals to solve a functional equation which is equivalent to the Stokes equation in the plane.

[a]This suggests that Nature has found, by inventing cilia, a way to circumnvent a "mathematical obstruction" for the efficiency of motion.

[b]Although the notations is coumbersome, we follow SW[1] notation for pourpouses of comparison.

It is well known that the Stokes equations in the plane are equivalen to the biharmonic equation $\Delta^4\Psi = 0$, see Bachelor[12] for instance. It is a elementary fact from complex function theory that biharmonic functions hav a representation in terms of analytic functions. SW use this representation t show that any solution can be written as

$$v(z, \bar{z}) = \phi(z) - z\overline{\phi'(z)} + \overline{\psi(z)} \tag{2}$$

where ϕ and ψ are analytical functions called *complex potentials* by similitud with Laplace equation in the plane. The boundary value problem for th Stokes equations is therefore equivalent to solving a functional equation wit boundary condition

$$V(s) = \phi(s) - s\overline{\phi'(s)} + \overline{\psi(s)} \tag{3}$$

where s is a coordinate on C. The point is to insert a boundary vector fiel into the lefthand side of (3), then find the analytic extensions of ϕ and ψ. For boundary values on the unit circle SW matched power series coefficient on both sides of (3). For conformal images of the circle the algebra become much more complicated, and the use of Cauchy integrals seems to be the best method of solution. The boundary data (3) pulled back to the unit circl under the transformation (1) takes the form

$$V(\sigma) = \phi(\sigma) - \frac{\omega(\sigma)}{\overline{\omega'(\sigma)}}\overline{\phi'(\sigma)} + \overline{\psi(\sigma)}. \tag{4}$$

The main tools for solving this functional equation are the following versions of Cauchy's theorem[11],

Corollary 1 *(Cauchy's theorem for infinite domains)*

$$\frac{1}{2\pi i}\oint_C \frac{f(z)dz}{z-\xi} = \begin{cases} -f(\xi) + f(\infty), & \xi \text{ outside } C \\ 0, & \text{otherwise} \end{cases} \tag{5}$$

for f analytic outside and continuous on C, a simple closed curve oriented counterclockwise.

Corollary 2 *A necessary and sufficient condition for the function f, continuous on the unit circle γ, to be the boundary condition of a function analytic outside γ is:*

$$\frac{1}{2\pi i}\oint_\gamma \frac{\overline{f(z)}dz}{z-\xi} = 0. \tag{6}$$

for all ξ outside γ.

The basic strategy of Muskhelishvili's method is to use Cauchy's theorem for infinite regions to eliminate one of the analytic functions ϕ or ψ, in order to determine the other function.

2.2 *Shapere-Wilczek's Connection and Curvature Forms*

Appealing to the Stokes paradox, a form of which states that the only solution to the Stokes equation corresponding to a rigid translation of a cylinder is a rigid translation of the fluid as a whole, Shapere and Wilczek asserted that the rotation and translation of the organism associated with a vector field $V(\sigma)$ on the boundary of the organism that generates a velocity field $v(z,\bar{z})$ can be determined from the asymptotics of that velocity field. Specifically

$$A^{rot}_{SW} = Im \oint_{lim|z|\to\infty} \frac{d\bar{z}}{2\pi i} v(z,\bar{z}), \tag{7}$$

and

$$A^{tr}_{SW} = \oint_{lim|z|\to\infty} \frac{dz}{2\pi i z} v(z,\bar{z}) \tag{8}$$

One of the purposes of our paper is to provide some corrections and clarifications to SW. It turns out that while formula for A^{tr} is correct, A^{rot} *is not* (unless C is a circle). We provide the corrections in section 4.

By the general theory of connections, the *curvatures* are the infinitesimal rigid motions $\mathcal{R}$ associated with traversing infinitesimal rectangles centered at C in shape space, spanned by the vectors ηV^h_n and ϵV^h_m. More precisely,

$$\mathcal{R}(\eta V^h_n, \epsilon V^h_m)\, C = e^{i\omega}\, C + b \tag{9}$$

where ω and b are written as

$$\begin{aligned} \omega &= A^{rot}([\eta v^h_n, \epsilon v^h_m]) \\ &\equiv \epsilon\eta F^{rot}_{mn} + \bar{\epsilon}\eta F^{rot}_{\bar{m}n} + \epsilon\bar{\eta} F^{rot}_{m\bar{n}} + \bar{\epsilon}\bar{\eta} F^{rot}_{\bar{m}\bar{n}}, \end{aligned} \tag{10}$$

and

$$\begin{aligned} b &= A^{tr}([\eta v^h_n, \epsilon v^h_m]) \\ &\equiv \epsilon\eta F^{tr}_{mn} + \bar{\epsilon}\eta F^{tr}_{\bar{m}n} + \epsilon\bar{\eta} F^{tr}_{m\bar{n}} + \bar{\epsilon}\bar{\eta} F^{tr}_{\bar{m}\bar{n}}. \end{aligned} \tag{11}$$

The reason for choosing this particular decomposition of the Stokes curvature form, as used by Shapere and Wilczek, will become evident in the examples. For the calculations, one makes the change of variable $z = \omega(\xi)$, in which A^{tr} becomes

$$A^{tr} = \oint_{lim|\xi|\to\infty} \frac{d\xi}{2\pi i \xi} v(\omega(\xi), \overline{\omega(\xi)}). \tag{12}$$

The expression for the Lie bracket pulled back to the ξ plane is

$$\begin{aligned} [V_n, V_m] &= (V_m \cdot \nabla) v_n - (V_n \cdot \nabla) v_m \\ &= (\frac{\partial v_n}{\partial \xi}\frac{\partial \xi}{\partial z})|_\gamma V_m + (\frac{\partial v_n}{\partial \bar{\xi}}\frac{\partial \bar{\xi}}{\partial \bar{z}})|_\gamma \bar{V}_m - (\frac{\partial v_m}{\partial \xi}\frac{\partial \xi}{\partial z})|_\gamma V_n \\ &\quad -(\frac{\partial v_m}{\partial \bar{\xi}}\frac{\partial \bar{\xi}}{\partial \bar{z}})|_\gamma \bar{V}_n. \end{aligned} \tag{13}$$

3 The Elliptical Swimmer (following the SW recipe)

We now compute the SW curvatures for the elliptical cylinder and apply th results to study swimming strategies for a nearly elliptical swimmer (we ca this kind of swimmer a *self deforming ellipse*). *It turns out that the rotation component according to SW's recipe is not correct.* We present it here for th sake of comparison with the corrected result in section 4).

The ellipse is given by the simplest conformal mapping, $m_1 = M$, all th others $m_i = 0$. In fact, the transformation

$$z = \omega(\xi) = R(\xi + \frac{M}{\xi}) \tag{14}$$

maps the region exterior to the unit circle γ in the ξ-plane to the regic exterior to the ellipse C with semi-axis $R(1+M)$ and $R(1-M)$.

The hodographed basis

$$v_n(z(\sigma)) = \lambda \sigma^{n+1}\,.$$

has a complicated explicit expression in the z-plane, namely, for

$$s = R\left(\exp(i\theta) + M\exp(-i\theta)\right),$$

we have

$$v_n(s) = \exp(i(n+1)\theta) \;=\; \lambda \left(\frac{s + \sqrt{s^2 - 4R^2M}}{2R}\right)^{n+1}.$$

Fortunately, the calculations in the ξ plane are feasible. The bounda condition for the ellipse corresponding to formula (4) takes the form

$$\phi(\sigma) - \frac{1}{\sigma}\frac{\sigma^2 + M}{1 - M\sigma^2}\overline{\phi'(\sigma)} + \overline{\psi(\sigma)} = \lambda\sigma^{n+1}, \tag{15}$$

Because the details of determining the solution to this equation parallel those found in Muskhelishvili in his computation of the stresses on a plate with an elliptical hole, will only state the results:

$$\phi(\xi) = \begin{cases} 0 & n > 1 \\ 0 & n = -1 \\ \lambda\xi^{n+1} & n < -1, \end{cases} \tag{16}$$

and

$$\psi(\xi) = \begin{cases} \bar{\lambda}\xi^{-n-1} & n > -1 \\ \bar{\lambda} & n = -1 \\ \xi\frac{(1+M\xi^2)}{(\xi^2-M)}(n+1)\lambda\xi^n & n < -1. \end{cases} \tag{17}$$

Substituting these into the formula for the $v_n(\xi)$ we obtain

$$\lambda v_n(\xi,\bar{\xi}) = \phi(\xi) - \frac{\bar{\xi}^2}{\xi}\frac{(\xi^2+M)}{(\xi^2-M)}\overline{\phi'(\xi)} + \overline{\psi(\xi)} \tag{18}$$

$$= \begin{cases} \lambda\bar{\xi}^{-n-1}, & n > -1 \\ \lambda, & n = -1 \\ \lambda\xi^{n+1} - (n+1)\frac{\bar{\xi}^2}{\xi}\frac{(\xi^2+M)}{(\xi^2-M)}\bar{\lambda}\bar{\xi}^n + \xi\frac{(1+M\bar{\xi}^2)}{(\xi^2-M)}(n+1)\bar{\lambda}\bar{\xi}^n, & n < -1 \end{cases}$$

Expressions (7) and (8) for the connection may now be used to decompose the boundary vector fields into horizontal and vertical parts.

Boundary Value	Horizontal Projection	Vertical Projection
$\lambda v_n(\sigma) = \lambda\sigma^{n+1}, n > 0$	$\lambda\sigma^{n+1}$	0
$\lambda v_0(\sigma) = \lambda\sigma$	0	$A^{rot} = Im\lambda$
$\lambda v_{-1}(\sigma) = \lambda$	0	$A^{tr} = \lambda$
$\lambda v_{-2}(\sigma) = \lambda\sigma^{-1}$	$\lambda\sigma^{-1} - ImM\lambda\sigma^{-1}$	$A^{rot} = ImM\lambda$
$\lambda v_n(\sigma) = \lambda\sigma^{n+1}, n < -2$	$\lambda\sigma^{n+1}$	0

(19)

Caveat: the results for the rotational part are not correct, see Proposion 3 in section 4.

To compute the Stokes curvature we compute the Lie bracket of horizontal vector fields, re-expand the resulting vector field in terms of the Fourier basis, then use the above table to determine the corresponding rigid rotation and translation. As an example if $m, n > -1$,

$$[\eta v_n, \epsilon v_m] = (\epsilon\bar{\eta}(m+1)\sigma^{m-n+1} - \bar{\epsilon}\eta(n+1)\sigma^{n-m+1})\sum_{k=0}^{\infty}(M\sigma^2)^k, \tag{20}$$

comparing this with the above table to determine the vertical components v find that for $m, n > -1$

$$F^{tr}_{m\bar{n}} = \begin{cases} (m+1)M^{\frac{j-1}{2}} & n-m=j>0 \\ & \text{and } j \text{ is odd} \\ 0 & \text{otherwise.} \end{cases} \tag{2}$$

$$F^{tr}_{\bar{m}n} = \begin{cases} (n+1)M^{\frac{k-1}{2}} & m-n=k>0 \\ & \text{and } k \text{ is odd} \\ 0 & \text{otherwise.} \end{cases} \tag{2}$$

$$F^{tr}_{mn} = F^{tr}_{\bar{m}\bar{n}} = 0 \tag{2}$$

For the circle $M = 0$ and the result of Shapere and Wilczek is recovere the only modes that couple are those that differ by one. If $M \neq 0$ all mod that differ by an odd number couple, although the strongest coupling tak place between ones that differ by just one. The effects of coupling betwe distant modes becomes more pronounced the further the shape is from a circ

3.1 Examples and discussion

Two examples will be presented, using only the translational part of the co nection (so that the previous calculations are correct). The first, an anal of the example of Blake's swimming circular cylinders[10], under symmetric deformations. The second example will be that of a long thin organism th swims utilizing the undulatory mode. The results of this model will be co pared with observations of the swimming motions of nematodes by Gray a Lissman.

For the first example consider an ellipse with semi-axis $1-M$ and $1+M$ and swimming stroke parameterized by:

$$S(\sigma,t) = (\sigma + \frac{M}{\sigma}) + (.025\cos 2\pi t)v_{14} + (.025\sin 2\pi t)v_{15} + (.015\cos 2\pi t)v_{18} + (.015\sin 2\pi t)v_{19} \tag{2}$$

To calculate the net translation of the swimmer the curvature compone corresponding to the coupling of modes 14 and 15, 14 and 19, 15 and 18, and and 19 are needed. After one swimming stroke the swimmer's net translati

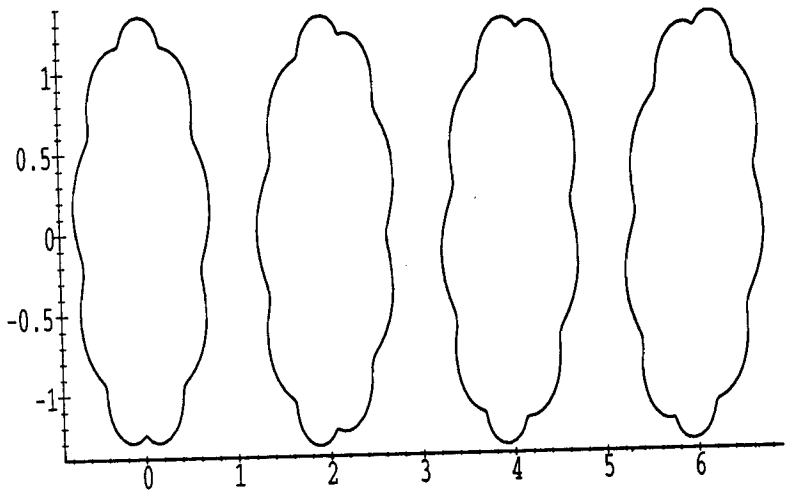

Figure 1. Ellipse (M = 3) at t=0, 0.25, 0.5, and 0.75

is given by:

$$\int_0^1 \mathcal{F}_{14,\overline{15}} a_{14}\bar{a}_{15}dt + \int_0^1 \mathcal{F}_{18,\overline{19}} a_{18}\bar{a}_{19}dt + \int_0^1 \mathcal{F}_{15,\overline{18}} a_{15}\bar{a}_{18}dt \qquad (25)$$

$$+ \int_0^1 \mathcal{F}_{14,\overline{19}} a_{14}\bar{a}_{19}dt$$

$$= .043 + .017M^2 - .019M \qquad (26)$$

See Figure 1.

Next, the undulatory mode of swimming will be studied by taking the eccentricity of the ellipse to be large and the deformations to have purely imaginary coefficients. Because this strategy is used by swimmers of all Reynolds numbers, this two dimensional model may provide a starting point for building models where the inertial forces are not negligible. J. Gray and H.W. Lissmann[7] conducted an extensive study of the various locomotion modes of Nematodes. They made observations and measurements of nematodes creeping on top of gelatin and damp glass, gliding through densely packed suspensions, and swimming through fluids. The present model will be applied to the latter class of nematodes, the *Turbatrix Acetii*. While swimming in an open fluid is clearly a three dimensional problem, the quantitative similarly between the two and three dimensional cases suggests that we might obta a reasonable model for the *Tubatrix* whose body motions were observed to essentially planar by Gray and Lissman.

The *Turbatrix Aceti* is a nematode which appears occasionally in domes vinegar. It has a body length of about $840\mu m$ and a diameter of 28μ Its ratio *length/width* ranges[13] about 45. It swims by passing undulato waves down its body. The observed wavelength was $712\mu m$, the frequen is 5.2 $\sec^{-1}$ or about one complete stroke every 1.9 seconds. The amplitu was measured to be approximately $107\mu m$ and observed speeds were 718μ per second, or $138\mu m$ per stroke. Thus the foreword progress was was abc 16.5% of the worms length per stroke.

To model the Tubatrix pick as the base shape an ellipse with semi-axis . and 1.94. Frequently the amplitude of the undulatory wave was observed increase as it passed down the body of the nematode, the tail moving nea four times as much as the head. This characteristic is related to the abil of the nematode to swim without yawing. The yawing motion associated t particular swimming stroke is not detected by the present model because side to side motion is zero on average. As a simple model, consider undulat swimming motions with a constant amplitude. The specific modes are cho to best represent the observations of Gray and Lissman (1963), see Figure The amplitude and ellipse size were chosen based on measurements of G and Lissman. Parametrize the swimmer by:

$$S(\sigma,t) = \sigma + \frac{0.94}{\sigma} + .17i\cos 2\pi t(v_3(\sigma)+v_{-5}(\sigma)) + .17i\sin 2\pi t(v_4(\sigma)+v_{-6}(\sigma$$

The deformations are transverse to the long axis of the ellipse, and the ove motion is purely translational. The curvature components corresponding the coupling of the modes 3 and 4, 3 and -6, -5 and 4, and -5 and are needed. In addition to formula (20) the following ones appear in computation of curvature components thorough,

$$\frac{\partial v_n}{\partial \xi}\frac{\partial \xi}{\partial z}v_m = \begin{cases} \sum_{k=0}^{\infty}(M\sigma^{-2})^k \epsilon\eta(n+1)\sigma^{m+n+1} \\ \quad -\sum_{k=0}^{\infty}(M\sigma^2)^k(n+1)\epsilon\bar{\eta}M\sigma^{m-n-1}, & n<-1 \\ 0, & n>-1 \end{cases}$$

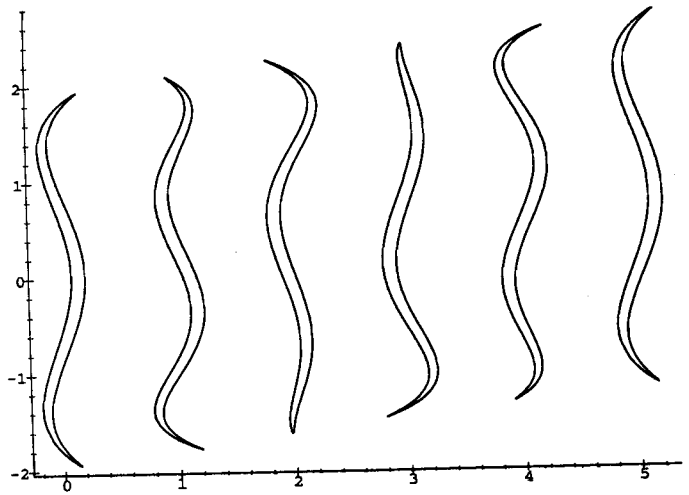

Figure 2. Locomotion of *Turbatrix aceti* at $t = 0, 0.2, 0.4, 0.6, 0.8$ and 1.0

$$\frac{\partial v_n}{\partial \bar{\xi}} \frac{\partial \bar{\xi}}{\partial \bar{z}} \bar{v}_m = \begin{cases} \left[\sum_{k=0}^{\infty} (M\sigma^2)^k\right]^2 \\ \quad \left((n+1)\bar{\epsilon}\bar{\eta} M \sigma^{-n-m-1} - (n+1)\bar{\epsilon}\bar{\eta}\sigma^{-n-m+1}\right), & n < -1 \\ \epsilon\bar{\eta}(m+1)\sigma^{m-n+1}, & n > -1. \end{cases}$$

The resulting curvature coefficients are: $F_{3,\bar{4}} = 4, F_{-6,-\bar{5}} = 4, F_{-\bar{5},\bar{4}} = 4M, F_{-5,4} = 4$, all other non-zero components being obtained by antisymmetry. The net translation is then found by computing:

$$\int_0^1 F_{3,\bar{4}} a_3(t)\dot{\bar{a}}_4(t)dt + \int_0^1 F_{-6,-\bar{5}} a_{-6}(t)\dot{\bar{a}}_{-5}(t)dt + \int_0^1 F_{-5,4} a_{-5}(t)\dot{a}_4(t)dt + \int_0^1 F_{-\bar{5},\bar{4}} \bar{a}_{-5}(t)\dot{\bar{a}}_4(t)dt. \tag{28}$$

The result of this integral is -0.71. After scaling, the predicted translation per stroke is $154\mu m$, or 18% of its length. Recall that the observed translations were approximately 16.5% of the length. The result seems quite good, in spite of the simplifications, namely: the model is two-dimensional; only four modes were excited, with constant amplitude; the correct Reynolds numb is of order 1, in the limit of applicability of Stokes approximation; effects order ≥ 3 in the amplitude were not taken into account.

4 Mathematical details and corrections to SW

4.1 The canonical vs. the hodographed Fourier basis

Suppose that in Goursat's representation for the solutions of planar Stol equations:

$$v(z) = \overline{\psi(z)} + \left(\phi(z) - z\overline{\phi'(z)}\right) \tag{3}$$

we take ψ and ϕ holomorphic in the exterior of the closed curve C. Witho loss of generality,

$$\phi = a_o + \frac{a_{-1}}{z} + \frac{a_{-2}}{z^2} + \dots \,.$$

$$\psi = \frac{b_{-1}}{z} + \frac{b_{-2}}{z^2} + \dots \tag{4}$$

The presence of a_o is a "confession of debt" to Stokes' paradox, si there is no solution vanishing at infinity for the translation of a cylinder.

Write

$$v(z) = \overline{\psi_o} + \sum_{k\leq 0}^{-\infty} \left(\sum_{\ell=1}^{4} v_k^{(\ell)}\right),$$

with

$$v_k^{(1,2)} = \overline{\psi_k(z)} = \begin{cases} v_k^{real} = \overline{z^k} \\ v_k^{Im} = i\overline{z^k} \end{cases}$$

$$v_k^{(3,4)} = \phi_k(z) - z\overline{\phi_k'(z)} = \begin{cases} w_k^{real} = z^k - kz\bar{z}^{k-1} \\ w_k^{Im} = i(z^k - kz\bar{z}^{k-1}) \end{cases}$$

Thus for each $k < 0$ we have four terms, taking for ψ and ϕ either z^k iz^k. This is called the *canonical basis*. Observe that v_k have good symme properties with respect to conjugation $z \to \bar{z}$ and reflection $z \to -z$. Howe w_k do not have these symmetries. This is already one good reason to susp that the canonical basis is not the best choice.

In Appendices A and B we obtain the curvatures for the circle, using canonical basis. in Appendix C we show that in the case of the ellipse, canonical basis does not allow a practical computation.

Let $z = z(\xi)$ the conformal map taking the exterior of $\gamma \equiv S^1$ to the exterior of C. We transport "hodographly" the Fourier basis $\{\sigma^{n+1}\}$ in γ to C, that is:

$$V_n(s) = (\xi(s))^{n+1}, \qquad n \in \mathbb{Z}.$$

We adopt the indexing $n \to n+1$ just to maintain the convention used by SW.

In contradistinction with the canonical basis, the symmetry properties are preserved by the hodographed Fourier basis. Suppose, for instance that C is symmetric with respect to the x-axis. Taking real coefficients, we produce symmetric deformations for all n. With imaginary coefficients, we get ondulating deformations.

The Fourier basis has other advantages. For *any* conformal map, half of the problem to find the Stokes extensions is trivial: for $n > -1$ we take *always* $\psi = \xi^{n+1}$ and $\phi \equiv 0$. As we will see in section 5, there are also remarkably simple properties for the power expenditure operator.

4.2 Total force and total torque

A simplified version of Stokes' paradox is given by the following

Lemma 1 *If the potentials ψ and ϕ have no singularities at ∞, as in (30) then the total force vanishes:*

$$\int_C f ds = 0$$

Proof. This follows from the identity

$$f ds = -2\mu i dU$$

where

$$U = \phi(z) + z\overline{\phi'} - \overline{\psi}\,.$$

In Appendix E we present a derivation of the force field

$$f = 4\mu Re(\phi' n) - 2\mu(z\overline{\phi''} - \overline{\psi'})\overline{n}\,. \tag{31}$$

Actually, Stokes' paradox implies that in order that the total force be $\neq 0$, the potential U must contain a logarithmic term. Following Blake[9], Shapere and Wilczek[1] avoided the logarithmic singularities altogether, using the following

Criterion 1 *Expand a vectorfield $v(z)$ along C with respect to the canonical basis (without logarithmic singularities). Then the translational component of the connection 1-form is the constant term $\overline{\psi_o}$.*

For the rotational component of the connection, we now present a correction[1] regarding the rotational part.

Criterion 2 *In dimension two the rotational part (as in dimension 3) is determined by the condition "total torque $T = 0$".*

In fact, we have

Lemma 2 *Using the canonical basis,*

$$T = 4\pi\mu Im[b_{-1}]$$

Proof. A simple calculation gives

$$tds = \mathrm{Im}[\overline{z}f]ds = -2\mu Re[\overline{z}dU] = -\mu dF$$

where

$$F = \overline{z}z(\overline{\phi'} + \phi') - z\psi - z\overline{\psi} + \xi + \overline{\xi}$$

e

$$\xi = \int_{z_o}^{z} \psi(z)dz$$

Observe that ξ is multivalued if $b_{-1} \neq 0$.

Remark 1 *The reader may feel unconfortable with the presence of the constant rigid translations of the fluid as a whole, which do not decay at infinit 1 and i as allowable vectorfields. Can one do differently? the answer is ye Translations of the shape can also be induced by stokeslets. However, the have even worse behaviour, logarithmic at infinity[14].*

Thus, in two-dimensions, one can still define translation-horizontality u ing the criterion "total force = 0", but this requires replacing the consta vectors 1 and i by the two stokeslets, on the x and y directions. In a futu work we plan to check if the criterion using stokeslets yields the same resul for the connection.

4.3 The 1-form of the connection

Given a velocity field $\vec{V}$ along C, we denote (a, b) the translation and $\omega\hat{k}$ t infinitesimal rotation such that

$$\vec{V} - \omega iz - (a, b)$$

is horizontal. First, we introduce terminology.

Definition 1 *If $(a, b) = (0, 0)$ we say $\vec{V}$ is translationally-horizontal. If ω 0 we say $\vec{V}$ is rotationally-horizontal.*

Along C, we expand $\overrightarrow{V}$ in terms of canonical components

$$v(z) = \overline{\psi_o} + \sum_{k\leq 0}^{-\infty}\sum_{\ell=1}^{4} v_k^{(\ell)} ,$$

(in practice, use a finite number, and approximate by least squares along C). The terms in $v_k, k < 0$ are translationally-horizontal, no matter the shape of C.

The translational component of the connection 1-form can be obtained from the asymptotics at infinity. Taking into account the decay of the elements of the canonical basis, one obtains

Theorem 1 (Shapere and Wilczek[1]). *Let $\hat{v}(z,\bar{z})$ be the Stokes extension of $v(s)$ along C. Then*

$$A^{tr} = \oint_{lim|z|\to\infty} \frac{dz}{2\pi i z}\hat{v}(z,\bar{z}) \tag{32}$$

SW argue that $v^h(s) = v(s) - \alpha(i\bar{z}^{-1})|_C$ with

$$\alpha = Im \oint_{lim|z|\to\infty} \frac{d\bar{z}}{2\pi i} v(z,\bar{z}) \tag{33}$$

is rotationally-horizontal. In other words, the rotational component of the connection, would be

$$A^{rot}_{SW} = \mathrm{Im} \oint_{lim|z|\to\infty} \frac{d\bar{z}}{2\pi i} v(z,\bar{z}), \tag{34}$$

This is not correct. Note that an infinitesimal rotation of C is (except for the circle), a combination of $i/\bar{z}$ with *other* elements of the canonical basis. Hence, for the rotational part, it is not sufficient to consider the single element $i/\bar{z}$ in the basis, corresponding to ψ_{-1} with imaginary coefficient. In other words, the flaw stems from the fact that, unless C is a circle, $i/\bar{z}|_C$ *does not represent an infinitesimal rotation* $R_C = iz|_C$.

4.4 Infinitesimal rotations: corrected formula

Consider a conformal transformation

$$z = \omega(\xi) = R(\xi + \frac{m_1}{\xi} + \cdots + \frac{m_n}{\xi^n})$$

from γ to a curve C (we can also take $n = \infty$). The following lemma is obvious.

Lemma 3 *The infinitesimal rotation with angular velocity $\omega = 1$, is given by*

$$iz(\xi) = iR(v_o + m_1 v_{-2} + \cdots + m_n v_{-(n+1)}) \tag{35}$$

where, in the right-hand side, $v_{-k} = \exp(i(-k+1)\theta)$ are elements of the hodographed Fourier basis.

For each

$$k = 0,\ k = -2,\ k = -(n+1) \ \ (k = -1 \text{ is absent}),$$

we must compute the Stokes extensions of the hodographed $v_k(s)$. Actually, for each k we need to find "only" the coefficient b^k_{-1} of ψ_k in the expansion of $\hat{v_k}$ in terms of the canonical basis. In the proposition below we omit the subscript -1 in the b^k's.

Proposition 1 *For indices*

$$k = 0,\ k = -2, \cdots, k = -(n+1),$$

the rotational part of the connection is given by:

$$A^{rot}(v_k) = \frac{1}{R}\frac{Im(b^k)}{Re(b^0 + m_1 b^{-2} \cdots + m_n b^{-(n+1)})} . \tag{36}$$

In fact, the vectorfields along C

$$v^h_k = v_k - \frac{Imb^k}{RRe(b^0 + m_1 b^{-2} \cdots + m_n b^{-(n+1)})} iR(v_o + m_1 v_{-2} + \cdots + m_n v_{-(n+1)}) \tag{37}$$

are rotationally-horizontal.

Conjecture 1 *Following Ken Meyer's talk in this Conference, our bet is 95%. All the remaining elements of the hodographed Fourier basis are rotationally horizontal (that is, for $k > 0$ and for $k < -(n+1)$). This involves finding the asymptotics of the Stokes extensions for the corresponding elements of the hodographed Fourier basis.*

We now give a more intrinsic version for (36). In order to obtain $A^{rot}(v) = \alpha$ we require that $(\hat{v} - \alpha iz)|_C$ produces zero total torque. Denote T the operator yielding the total torque. From $T(v - \alpha iz) = 0$ we get $\alpha = T(v)/T(iz)$.

Theorem 2

$$A^{rot}(v) = \frac{2\mu}{T_C}\lim_{R\to\infty} Im\left(\frac{1}{2\pi i}\oint_{|z|=R} \hat{v}(z)\, d\bar{z}\right),$$

where $T_C = T(iz)$ is the torque associated to the infinitesimal rotation $iz(z)$ of C.

4.5 The ellipse. Rotational components.

We saw, in section 3 the expressions for the Stokes extensions $\phi(\xi)$ and $\psi(\xi)$ of the Fourier modes. We can write, for $|\xi| > 1$,

$$\phi_k(\xi) = a_0^k + \frac{a_{-1}^k}{R\xi} + \cdots,$$

$$\psi_k(\xi) = \frac{b_{-1}^k}{R\xi} + \cdots.$$

We are interested in finding which k have nonvanishing coefficients b_{-1}^k. We claim that only $v_{0,\lambda}$ and $v_{-2,\lambda}$ do have them. In fact, since

$$\psi(\xi) = \begin{cases} \frac{\bar{\lambda}}{\xi} = \frac{\bar{\lambda}R}{R\xi} & ,n=0 \\ -\frac{M\lambda}{\xi}\frac{\xi^2+M^{-1}}{\xi^2-M} = -\frac{M\lambda R}{R\xi} + \cdots & ,n=-2 \end{cases}$$

(omitting the superscripts k)

it follows that the only nonvanishing b_{-1}^k occur for $k=0$ and $k=-2$. Hence

Lemma 4 *The following expression for the total torque holds*

$$\frac{T(v_{0,\lambda})}{4\pi\mu} = Im(R\bar{\lambda}) = -RIm(\lambda),$$

$$\frac{T(v_{-2,\lambda})}{4\pi\mu} = -MRIm(\lambda),$$

in particular the rotational components of the connection are

$$A^{rot}(\lambda v_0) = -\frac{4\pi\mu R}{T_C}Im(\lambda), \qquad A^{rot}(\lambda v_{-2}) = -\frac{4\pi\mu MR}{T_C}Im(\lambda).$$

To compute T_C, we consider the infinitesimal rotation $iz|C = iz(C)$. The Stokes extension is given by:

$$\widehat{iz(C)} = iR(\widehat{\sigma + M\sigma^{-1}}) = \widehat{iR\sigma} + \widehat{iRM\sigma^{-1}} = \widehat{v_{0,iR}(\sigma)} + \widehat{v_{-2,iRM}(\sigma)}.$$

Thus the infinitesimal rotation of the ellipse requires two elements from the hodographed Fourier basis, precisely those having coefficient s $b_{-1}^k \neq 0$. Now,

$$\begin{aligned}\psi(\xi) &= -\frac{iR}{\xi} - \frac{iRM^2}{\xi}\frac{\xi^2+M^{-1}}{\xi^2-M} \\ &= -\frac{iR^2}{R\xi} - \frac{iR^2M^2}{R\xi} + \cdots \\ &= -\frac{iR^2(1+M^2)}{\xi} + \cdots.\end{aligned}$$

Lemma 5 *The total torque associated to the infinitesimal rotation $T(iz)$ the ellipse is*

$$T_C = -4\pi\mu R(1+M^2).$$

substituting the above expression in the expression for the rotational comp nents of the connection yields

Proposition 2 *The rotational components of the connection at the basis e ements $v_{0,\lambda}$ and $v_{-2,\lambda}$ are*

$$A^{rot}(v_{0,\lambda}) = \frac{Im(\lambda)}{R(1+M^2)} \equiv \omega_0,$$

$$A^{rot}(v_{-2,\lambda}) = \frac{MIm(\lambda)}{R(1+M^2)} \equiv \omega_{-2}.$$

in particular the following decomposition into rotationally-horizontal ar purely rotational components holds

$$v_{0,\lambda}^h(\sigma) = \left(\lambda - i\frac{Im(\lambda)}{1+M^2}\right)\sigma - i\frac{Im(\lambda)}{1+M^2}\sigma^{-1},$$

$$v_{-2,\lambda}^h(\sigma) = \left(\lambda - i\frac{M^2Im(\lambda)}{1+M^2}\right)\sigma - i\frac{MIm(\lambda)}{1+M^2}\sigma^{-1}$$

Summarizing:

Theorem 3 *Given*

$$v(\sigma) = \sum v_{n,\lambda_n}(\sigma) = \sum \lambda_n \sigma^{n+1}$$

along the ellipse. Then

$$A^{tr}(v) = \lambda_{-1},$$

$$A^{rot}(v) = \frac{Im(\lambda_0)}{R(1+M^2)} + \frac{MIm(\lambda_{-2})}{R(1+M^2)}.$$

The rotational components of the curvatures can be computed in a simila fashion as in section 3, finding the b_{-1} residues in the Lie brackets.

5 Power expenditure

5.1 The differential form $fds = gd\theta$

Forces can be represented by the same space $\mathcal{V}_C$ of velocity vectorfields alon C, with the L^2 norm. Intrinsically, however, it is an abuse to consider

$$2\mu f = 2\mu\left(2Re(\phi' n) + (\overline{\psi'} - z\overline{\phi''})\overline{n}\right) \qquad (38$$

as an element of $\mathcal{V}_C$. Actually, the stress force is a *differential form* $f\,ds$, where s is arclength parameter along the curve C. It belongs to the *dual* space $\mathcal{V}^*$. In what follows we use the notation $f = f(v(s))$ for the vector of forces associated to the vector of velocities $v(s)$ along C. We now explore (to our benefit) the possibility of *not* identifying these spaces. We use the pull-backs of the forces *as forms* to γ, under the conformal mapping $z = z(\xi)$ sending the exterior of the γ to the exterior of C.

Proposition 3 *Let s be the arc length parameter along the curve C, and θ the polar angle in the unit circle corresponding under the conformal mapping $z = z(\xi)$. Let $f = f(v(s))$ be the vector of forces associated to the vector of velocities with complex potentials ϕ, ψ, and let $g\,d\theta$ denote the pullback of the differential form $f\,ds$ to the unit circle, so $f\,ds = g\,d\theta$, then*

$$g = I + II + III + IV + V \tag{39}$$

where

$$\begin{aligned}
I &= \overline{\frac{d\psi}{d\xi}}\,\sigma^{-1} \\
II &= \frac{d\phi}{d\xi}\sigma \\
III &= \left(\overline{\frac{d\phi}{d\xi}}\right)\frac{dz/d\xi}{\overline{dz/d\xi}}\,\sigma \\
IV &= -\frac{z(\xi)\sigma^{-1}\,\overline{d^2\phi/d\xi^2}}{\overline{dz/d\xi}} \\
V &= z(\xi)\sigma^{-1}\frac{\overline{d\phi/d\xi}\;\overline{d^2z/d\xi^2}}{(\overline{dz/d\xi})^2}.
\end{aligned} \tag{40}$$

The proof is a long but straightforward calculation, using the chain rule and taking into account that $\xi = \sigma = \exp(i\theta)$ along γ. Since we are using hodographed velocity fields $v(\sigma)$ from γ to C, the power expenditure is given by the usual inner product

$$\mathcal{P} = 2\mu\int_\gamma (v, g)\,d\theta.$$

where now we identify $gd\theta$ with the vector field $g \in \mathcal{V}_\gamma$, the space of vector fields along γ.

Lorentz reciprocity[14] carries over to this representation, in other words, the operator

$$\mathcal{P}^\gamma : \mathcal{V}_\gamma \to \mathcal{V}_\gamma, \quad v \mapsto g. \tag{41}$$

is self-adjoint and positive. If we could determine the spectrum of $\mathcal{P}^\gamma$, then the task of computing power expenditures would be completely solved. We assert that one of the advantages of the hodographed basis is that half of the spectral problem is a free lunch!

In fact, for $n \geq -1$ we know that

$$\psi = \xi^{-(n+1)}\ ,\ \phi \equiv 0\ .$$

hence

$$v = \overline{\sigma}^{-(n+1)} = \sigma^{n+1}$$

and

$$g = \overline{\frac{d\psi}{d\xi}}\,\sigma^{-1} = -(n+1)\overline{\xi^{-(n+2)}}\sigma^{-1} = -(n+1)\,\sigma^{n+2}\,\sigma^{-1} = -(n+1)\sigma^{n+1}$$

Theorem 4 *For every conformal mapping $z = z(\xi)$, if $n + 1 > 0$, then σ^{n+1} is an eigenvalue of $\mathcal{P}^\gamma$, with eigenvector $-(n+1)$.*

It is interesting to look what happens geometrically in the physical z-plane. The force field $f \in \mathcal{V}_C$, is parallel (with opposing sense) to the velocity field $v(z(\sigma)) = \sigma^{n+1}$. The scale factor depends on the conformal mapping,

$$f = -(n+1)\,\frac{\sigma^{n+1}}{ds/d\theta}$$

To compute the power expenditure $\mathcal{P}$, the scale factor disappears when we change the integration to γ.

The difficult part of the spectral problem involves only the indices $n + 1 < 0$. The following proposition shows that they form an invariant subspace.

Teorem 5 *The operator $\mathcal{P}^\gamma(v) = g$ leaves invariant the subspace of negative Fourier modes σ^{n+1}.*

Proof. Use Lorentz reciprocity. Let $m \geq 0$; then

$$(\mathcal{P}(\sigma^{n+1})\,,\,\sigma^m) = (\mathcal{P}(\sigma^m)\,,\,\sigma^{n+1}) = \int_\gamma -m\sigma^m\,\sigma^{n+1}d\theta = 0$$

5.2 Computing g for the ellipse; negative Fourier modes

Recall that for $p < -1$

$$\phi = \lambda \xi^{p+1} \ , \ \psi = \lambda(p+1)\xi^{p+1}\frac{1+M\xi^2}{\xi^2 - M}$$

We insert in (39-40). In the denominators appear factors $1-M\sigma^2$, coming from the derivatives of $z(\xi)$ and $\xi^2 - M$, followed by conjugation (remember $\overline{\sigma} = \sigma^{-1}$). Well, for $0 < M < 1$

$$\frac{1}{1-M\sigma^2} = \sum_{n=0}^{\infty} M\sigma^{2n} \ .$$

We know, however, that in the final result for g, only negative powers of C do appear. The term

$$II = \frac{d\phi}{d\xi}\sigma = \lambda(p+1)\sigma^{p+1}$$

is in accordance, but the terms. I, III, IV, V are problematic. Nonetheless, a "miracle" occurs:

Lemma 6 *For the conformal mapping $z = R(\xi + M/\xi)$ of the exterior of unit circle onto the exterior of the ellipse C, let $f(\lambda\sigma^{p+1})$ denote the vector of forces associated to the hodographed vector field $\lambda v_{p+1}(\sigma) = \lambda\sigma^{p+1}$, let $g\,d\theta$ denote the pullback of the differential form $f\,ds$ to the unit circle, so $f\,ds = g\,d\theta$ (see Proposition 3), then $I + III + IV + V \equiv 0$, in particular for $p + 1 < 0$,*

$$f(\lambda\sigma^{p+1})\,ds = \lambda(p+1)\sigma^{p+1}\,d\theta.$$

Proof. A direct calculation.

Theorem 6 *For the ellipse, the hodographed vector fields $v(\sigma) = \sigma^{p+1}$ for $p+1 < 0$ are also eigenvectors of $\mathcal{P}^\gamma : v \to g$, with eigenvalue $p+1$.*

We think that this is indeed remarkable: when we vary the eccentricity $0 < M < 1$, using the hodographed Fourier basis, the power expenditure functional does not change!

5.3 Hypotrochoids

The degree of algebraic difficulty increases, but we can still calcultate, $g(\lambda\sigma^{p+1})d\theta$ for the hypotrochoids[11]

$$z = R\left(\xi + \frac{M}{\xi^m}\right), \tag{42}$$

with $m = 1, 2, \ldots$, and M a positive constant satisfying $0 < mM < 1$.

We present the results:

Theorem 7 *Consider the hodographed Fourier basis $v_n(\sigma) = \sigma^{n+1}$ under the conformal mapping (42). Then*

1. *For any $m \in \mathbb{N}$, and $n + 1 \geq 0$ $v_n(\sigma) = \sigma^{n+1}$ is an eigenvalue of the Lorentz operator $\mathcal{P}^\gamma$ (see 41) with eigenvalue, $-(n+1)$.*
2. *For $m = 2$ and $n + 1 < 0$ the "miracle" (see Lemma (6)) still holds, namely if $f\,ds = g\,d\theta$ is the pullback ot the form of forces and $g = I + II + III + IV$, asi in (40), then $I + III + IV + V \equiv 0$.*
3. *For $m = 3$ and $p + 1 < 0$ the same "miracle" holds, except for $p = -2$, here for the hodographed vector field $\lambda v_{-2}(\sigma) = \lambda\sigma^{-1}$,*

$$g(\lambda\sigma^{-1}) = (-\beta + M\overline{\beta})\sigma^{-1} \ , \ \beta = \frac{\lambda - M\overline{\lambda}}{1 - M^2}$$

so the eigenvalue is different from the others.

4. *For $m = 4$ we found*

$$g(\lambda\sigma^{-1}) = -\lambda\,\sigma^{-1} + \overline{\lambda}\sigma^{-2}$$

Here the hodographed Fourier basis is not an orthogonal basis for the power expenditure operator.

6 Efficiency of an elliptic microswimmer

There are basically two competing efficiency notions for microswimming. Consider a swimming stroke of period τ, in shape space $\mathcal{S}$ and the ratio

$$\frac{X}{E} = \frac{X/\tau}{E/\tau} = \frac{\text{mean velocity}}{\text{mean power}} \ . \tag{43}$$

Froude's efficiency is an non-dimensional quantity which results from multiplying this ratio by a "characteristic force" $\bar{T}$, and in the Stokesian realm it is equivalent (up to a shape dependent factor) to *Lighthill's efficiency*

$$\text{ef}_L = \frac{(\text{mean velocity})^2}{\text{mean power}} \ . \tag{44}$$

The other notion, which we call *SW efficiency* (because Shapere and Wilczek essentially use it) is given by

$$\text{ef}_{SW} = \frac{X}{\tau E} \ , \tag{45}$$

where the presence τ in the denominator is equivalent to consider all swimming strokes with period $\tau = 1$. In this paper we will consider the latter notion, and consider a variational problem first introduced by Shapere and Wilczek leading to the most efficient strokes. For a comparison of the two notions, see[15].

6.1 *The variational problem*

We expand the time-dependent, small shape deformations in terms of a basis, so that the problem is linearized to a Lagrangian

$$\mathcal{L} = \frac{1}{2}(\mathcal{K}\dot{q}, \dot{q}) - \nu\frac{1}{2}(\mathcal{F}q, \dot{q}) \ , \tag{46}$$

where the matrix K encodes the power expenditure, F the curvatures, ν is a Lagrange multiplier. The Euler-Lagrange equations are

$$\mathcal{K}\dot{q} = \nu\mathcal{F}q \ . \tag{47}$$

In other words, $\mathcal{L}$ describes the problem of minimizing the energy expenditure

$$E = \frac{1}{2}\int_0^\tau (\mathcal{K}\dot{q}, \dot{q})dt \ ,$$

for a prescribed holonomy

$$X = \frac{1}{2}\int_0^\tau (\mathcal{F}q, \dot{q})dt \ .$$

Inserting

$$q = \epsilon V e^{i\Omega t} \ , \tag{48}$$

where V is an eigenvector, gives

$$\mathcal{F}V = \lambda\mathcal{K}V \ , \ \lambda = \frac{i\Omega}{\nu} \tag{49}$$

Define

$$W = \mathcal{K}^{\frac{1}{2}}V \ , \ \mathcal{B} = \mathcal{K}^{-\frac{1}{2}}\mathcal{F}\mathcal{K}^{-\frac{1}{2}} \text{ skewsymmetric,} \tag{50}$$

so that:

$$\mathcal{B}W = \lambda W \ . \tag{51}$$

Taking into account that $\tau = 2\pi/\Omega$, the efficiency can be written as

$$\text{ef} = \frac{X\Omega}{E} \ , \tag{52}$$

where we omit the factor 2π. Some simple manipulations with E and X give

$$E = \frac{1}{2}\Omega^2\epsilon^2(\mathcal{K}V, V)\tau$$

$$X = -\frac{i}{2}\Omega\epsilon^2(\mathcal{F}V, V)\tau \ .$$

Since $\mathcal{F}V = \lambda\mathcal{K}V$, we get

$$\text{ef} = \frac{X\Omega}{E} = -i\lambda \ , \tag{53}$$

Recall that $\lambda = i\Omega/\nu$ is an eigenvalue of (51), and as expected, it is purely imaginary. In short: *Finding SW's efficiency is equivalent to find the supremum of the purely imaginary spectrum.*

6.2 *Numerical results*

For the elliptical swimmer, undergoing symmetric swimming strokes, matrices K and F are given in Appendix F. We found the spectrum using *MathLab*, for $M = 0$ (circle), $M = 0.1$ e $M = 0.2$ (ellipses with small eccentricity) and $M = 0.8$ e $M = 0.9$ (high eccentricity).

Regarding the number of Fourier modes, we solved the problem exciting the first five, the first ten, the first 30, and finally the ten modes between 30 and 39. Tables of results are available upon request.

Our observations are as follows. As expected, the absolute values increase as more modes are considered. Interestingly, they do not diminish significantly as we exclude the lower Fourier modes. This indicates, as shown by SW for the circle and the sphere, that the more efficient strokes involve essentially the high geometric modes.

In the table below we list the highest eigenvalues (51), for small and for high eccentricities.

	$M = 0$	$M = 0.1$	$M = 0.2$	$M = 0.8$	$M = 0.9$
First 5 modes	1.9906i	1.9664i	1.9431i	2.4541i	2.7878i
First 10 modes	2.4008i	2.2845i	2.1826i	3.3162i	4.2483i
First 30 modes	2.7016i	2.4884i	2.3139i	4.9168i	7.2448i
10 modes, from 30 to 39	2.6529i	2.4717i	2.3134i	4.0299i	5.6556i

We have also considered very high order modes, between 30000 e 30009, and we verified that there seems to exist a higher bound for all efficiencies, as conjectured by SW[2] .

The advantage of high order geometric modes supports Nature's choice for ciliary motion rather than deformations of a membrane. The mechanical stress would be too strong for a membrane undergoing high order deformations. On the other hand, it is quite easy to a ciliary envelope to emulate these motions.

Acknowledgments

Thanks to LNCC/CNPq for supporting a scientific visit of one of the authors (J.D.) to Rio de Janeiro, February 1998.

Appendix

A. The Lie bracket

Let $z = x + iy$, $\overline{z} = x - iy$. Denote

$$\frac{\partial}{\partial z} = \frac{1}{2}\left(\frac{\partial}{\partial x} - i\frac{\partial}{\partial y}\right) \ , \ \frac{\partial}{\partial \overline{z}} = \frac{1}{2}\left(\frac{\partial}{\partial x} + i\frac{\partial}{\partial y}\right).$$

A vector field

$$\vec{v} = (a(x,y), b(x,y)) = a\frac{\partial}{\partial x} + b\frac{\partial}{\partial y}$$

is represented as

$$v = f\frac{\partial}{\partial z} + \overline{f}\frac{\partial}{\partial \overline{z}}$$

where $f = a(x,y) + ib(x,y) = f(z,\overline{z})$.

Lemma 7 *The Lie bracket $\vec{w} = [\vec{u}, \vec{v}]$ can be computed as follows:*

$$w = [u,v] = \begin{bmatrix} g_z & g_{\overline{z}} \\ \overline{g}_z & \overline{g}_{\overline{z}} \end{bmatrix} \begin{bmatrix} f \\ \overline{f} \end{bmatrix} - \begin{bmatrix} f_z & f_{\overline{z}} \\ \overline{f}_z & \overline{f}_{\overline{z}} \end{bmatrix} \begin{bmatrix} g \\ \overline{g} \end{bmatrix} \tag{54}$$

or as

$$w = h\frac{\partial}{\partial z} + \overline{h}\frac{\partial}{\partial \overline{z}},$$

with

$$h = g_z f + g_{\overline{z}}\overline{f} - f_z g - f_{\overline{z}}\overline{g}. \tag{55}$$

Consider, for $n, m < 0$, the vectorfields

$$v_n = \overline{z}^n \ , \ u_m = z^m - mz\overline{z}^{m-1}$$

written as differential operators as

$$v_n = \overline{z}^n\frac{\partial}{\partial z} + z^n\frac{\partial}{\partial \overline{z}}$$

$$u_m = (z^m - mz\overline{z}^{m-1})\frac{\partial}{\partial z} + (\overline{z}^m - m\overline{z}z^{m-1})\frac{\partial}{\partial \overline{z}}.$$

We obtain

$$[v_n, v_p] = pz^n\overline{z}^{p-1} - nz^p\overline{z}^{n-1}. \tag{56}$$

Curvatures for the circle

For the circle $S_a : r = a$, the translational component of the curvature is the constant term in the Fourier expansion of these brackets alongo S_a. For $n < p < 0$ we get

$$\begin{aligned} F^{tr}(v_n, v_p) &= a^{n+p}F^{tr}(\sigma^{|n|}, \sigma^{|p|}) = \\ &= \frac{1}{2\pi}\int_0^{2\pi}[v_n, v_p]d\theta = \\ &= \frac{a^{n+p-1}}{2\pi}\int_0^{2\pi}\left(p\,e^{(n-p+1)i\theta} - n\,e^{(p-n+1)i\theta}\right)d\theta. \end{aligned}$$

Just the first integral can contribute, and only if $p = n+1$, so that

$$F^{tr}(\sigma^{|n|}, \sigma^{|p|}) = \frac{n+1}{a}\ . \tag{57}$$

B. Curvatures for the ellipse using the canonical basis

The ellipse

$$\frac{x^2}{a^2} + \frac{y^2}{b^2} = 1$$

is described in polar coordinates by $r = r(\theta)$, with

$$r = \left(\frac{\cos^2\theta}{a^2} + \frac{\sin^2\theta}{b^2}\right)^{-1/2}\ . \tag{58}$$

It is possible, but not practical, to compute directly the curvature coefficients using the canonical basis. Let's see why. To compute $F_{trans}(v_n, v_p)$, we substitute (58) in (56). The two terms have the same absolute value,

$$\left(\frac{\cos^2\theta}{a^2} + \frac{\sin^2\theta}{b^2}\right)^{-(p+n-1)/2}$$

but different phases

$$\exp(i(n-p+1)\theta) \text{ and } \exp(i(p-n+1)\theta)\,.$$

As a working hypothesis, suppose we will have only $p+n$ odd (recall $p+n$ is < 0). The situation is not completely desperate, since the absolute values as well as the phases are trigonometric polynomials. We must now expand the bracket in the basis $\{v_n, w_n\}$. Assuming that we need just the even negative n's, we mould get finite trigonometric expressions on both sides. However, finding the coefficients of the expansion becomes a very complicated combinatorial-matricial problem.

C. Ellipse using the Fourier basis. More details.

Lie brackets

In the text we only gave the case $m, n < -1$. For $m < -1$ and $n > -1$ we have:

$$\begin{aligned}[\lambda_n v_n, \lambda_m v_m] = \sum_k \frac{\lambda_n \bar{\lambda}_m}{R}(m-n)M^k\sigma^{n-m+1+2k} - \\ -\sum_k \frac{\lambda_n\lambda_m}{R}(m+1)M^k\sigma^{n+m+1-2k} \\ +\sum_k \frac{\bar{\lambda}_n\bar{\lambda}_m}{R}(m+1)(k+1)M^k\sigma^{-n-m+1+2k} - \\ -\sum_k \frac{\bar{\lambda}_n\bar{\lambda}_m}{R}(m+1)(k+1)M^{k+1}\sigma^{-n-m-1+2k}\end{aligned}$$

For $m, n < -1$ one gets

$$\begin{aligned}[\lambda_n v_n, \lambda_m v_m] = \sum_k \frac{\lambda_n\lambda_m}{R}(n-m)M^k\sigma^{n+m+1-2k} + \\ +\sum_k \frac{\bar{\lambda}_n\bar{\lambda}_m}{R}(n-m)(k+1)M^{k+1}\sigma^{-n-m-1+2k} \\ +\sum_k \frac{\bar{\lambda}_n\bar{\lambda}_m}{R}(m-n)(k+1)M^k\sigma^{-n-m+1+2k} + \\ +\sum_k \frac{\lambda_n\bar{\lambda}_m}{R}(m+1)M^k\sigma^{n-m+1+2k} - \\ -\sum_k \frac{\bar{\lambda}_n\lambda_m}{R}(n+1)M^k\sigma^{-n+m+1+2k}\end{aligned}$$

D. Formula for the Force f

Given a closed curve C, we denote the exterior normal by

$$n = -i\frac{dz}{ds}$$

where s is the arclength, traversed counterclockwise.

Proposition 4

1. *The pressure is given by*

$$p = -4\mu Re[\phi'] \tag{59}$$

2. *The stress force at $z \in C$ is*

$$f = 4\mu Re(\phi' n) - 2\mu(z\overline{\phi''} - \overline{\psi'})\,\overline{n}\ . \tag{60}$$

3. *The differential form $f ds$ can be written as*

$$f ds = -2i\mu\left\{(\phi' + \overline{\phi'})dz + (z\overline{\phi''} - \overline{\psi'})d\overline{z}\right\} \tag{61}$$

Proof. We start with $\psi = f + ig$. The velocity components are $u = f$ and $v = -g$. Since f and g are harmonic, $\Delta u = \Delta v \equiv 0$, Stokes equations are satisfied with pressure $p \equiv 0$. We compute the stress tensor:

$$e_{11} = f_x = \frac{1}{2}(f_x + g_y)$$

$$e_{12} = \frac{1}{2}(f_y - g_x) = f_y = -g_x$$

$$e_{22} = -g_y = -\frac{1}{2}(f_x + g_y)$$

We write the normal vector as $n = p + iq$. Then

$$\begin{aligned}\begin{pmatrix} e_{11} & e_{12} \\ e_{21} & e_{22}\end{pmatrix}\cdot\begin{pmatrix} p \\ q\end{pmatrix} &= \begin{pmatrix} f_x & f_y \\ f_y & -f_x\end{pmatrix}\cdot\begin{pmatrix} p \\ q\end{pmatrix} = \\ &= \begin{pmatrix} f_x & -f_y \\ f_y & f_x\end{pmatrix}\cdot\begin{pmatrix} p \\ -q\end{pmatrix} = \\ &= (e_{11} + ie_{12})(p - iq) = \overline{\psi'}\,\overline{n}\end{aligned}$$

Now we compute with $\phi = F + iG$. The components of $u + iv = \phi - z\overline{\phi'}$ are

$$u = F - xF_x - yG_x$$
$$v = G + xG_x - yF_x$$

A short calculation gives

$$u_x = -xF_{xx} - yGxx$$
$$u_y = F_y - xF_{xy} - G_x - yG_{xy}$$
$$v_x = 2G_x + xG_{xx} - yF_{xx}$$
$$v_y = xG_{xy} - yF_{xy}$$

using one the the Cauchy-Riemann equations, namely $F_x = G_y$. Using the other one, $F_y = -G_x$ we obtain:

$$\Delta u = -4F_{xx}\,, \Delta v = -4F_{xy}\,.$$

Hence, the pressure is

$$p = -4\mu F_x = -2\mu(\phi' + \overline{\phi'}),$$

and the components of the stress tensor are:

$$e_{11} = -xF_{xx} - yGxx$$
$$e_{22} = xG_{xy} - yFxy \quad (e_{11} = -e_{12})$$
$$e_{12} = \frac{1}{2}(v_x + u_y) = -xF_{xy} - yF_{xx}$$

In complex variables notation

$$e_{11} + ie_{12} = -\overline{\phi''}\, z$$

so that the force associated to ϕ is

$$-2\mu\overline{\phi''}\, z\, \overline{n} + 2\mu(\phi' + \overline{\phi'})\, n$$

Everything together yields

$$f = 2\mu\overline{\psi'}\, \overline{n} - 2\mu\overline{\phi''}\, z\, \overline{n} + 2\mu(\phi' + \overline{\phi'})n$$

E. Matrices K and F for the elliptic swimmer

We consider symmetric deformations, so all $\lambda_n = 1$.

Curvatures

$n\backslash m$	0	1	−2	2	−3	3	−4	4
0	0	$-\frac{1}{R}$	0	0	0	$-\frac{M}{R}$	0	0
1	$\frac{1}{R}$	0	$\frac{M+1}{R}$	$-\frac{2}{R}$	0	0	0	$-\frac{2M}{R}$
−2	0	$-\frac{M+1}{R}$	0	0	$\frac{1}{R}$	$-\frac{2M^2+M-1}{R}$	0	0
2	0	$\frac{2}{R}$	0	0	$2\frac{M+1}{R}$	$-\frac{3}{R}$	0	0
−3	0	0	$-\frac{1}{R}$	$-2\frac{M+1}{R}$	0	0	$\frac{2}{R}$	$-2\frac{2M^2+M-1}{R}$
3	$\frac{M}{R}$	0	$\frac{2M^2+M-1}{R}$	$\frac{3}{R}$	0	0	$3\frac{M+1}{R}$	$-\frac{4}{R}$
−4	0	0	0	0	$-\frac{2}{R}$	$-3\frac{M+1}{R}$	0	0
4	0	$-\frac{2M}{R}$	0	0	$2\frac{2M^2+M-1}{R}$	$\frac{4}{R}$	0	0

Power expenditures

$n\backslash m$	0	1	−2	2	−3	3	−4	4
0	1	0	0	0	0	0	0	0
1	0	2	0	0	0	0	0	0
−2	0	0	1	0	0	0	0	0
2	0	0	0	3	0	0	0	0
−3	0	0	0	0	2	0	0	0
3	0	0	0	0	0	4	0	0
−4	0	0	0	0	0	0	3	0
4	0	0	0	0	0	0	0	5

References

1. A. Shapere and F. Wilczek, Geometry of self-propulsion at low Reynolds number, *J.Fluid Mech.* **198**, 557–585, (1989).
2. A. Shapere and F. Wilczek, Efficiencies of self-propulsion at low Reynolds number, *J.Fluid Mech.* **198**, 587–599, (1989).
3. J. Koiller, R. Montgomery and K. Ehlers, Problems and progress in Microswimming, *J. Nonlinear Science* **6**, 507–541, (1996).
4. K.M. Ehlers, The Geometry of Swimming and Pumping at Low Reynolds number, *PhD Thesis*, Univ. of Calif., Santa Cruz (1995).
5. A. Cherman, *M.Sc. thesis*, Centro Brasileiro de Pesquisas Físicas, (1998).
6. K. Ehlers, in preparation.
7. J. Gray and H.W. Lissmann, The Locomotion of Nematodes, *J. Explt. Biol.*, **41**, 135–154, (1964).
8. J. Lighthill, On the squirming motion of nearly spherical deformable bodies through liquids at very small Reynolds number, *Commun. Pure Appl. Math.* **5**, 109–118, (1952).
9. J. R. Blake, A spherical envelope approach to ciliary propulsion, *J.Fluid Mech.* **46**, 199–208, (1971).
10. J.R. Blake, Self propulsion due to oscillations on the surface of a cylinder at low Reynolds number, *Bull.Austral.Math.Soc.***3**, 255–264, (1971).
11. N.I. Muskhelishvili, Some basic problems of the mathematical theory of elasticity, P.Noordhoff, Groningen-Holland, (1953).
12. G.K. Batchelor, An introduction to Fluid Mechanics, Cambridge University Press, (1970).
13. D.B. Dusenbery, Life at Small Scale, Scientific American library, (1996).
14. C. Pozrikids, Boundary Integral and Singularity Methods for Linearized Viscous flow, Cambridge Texts in Applied Mathematics, 1992.
15. J. Koiller and J. Delgado, On efficiency calculations for nonholonomic locomotion systems, *Reports Math. Phys.*, **42**, 165–183, (1998).

2–DIMENSIONAL INVARIANT TORI FOR THE SPATIAL ISOSCELES 3–BODY PROBLEM

MONTSERRAT CORBERA

Departament de Física i Matemàtica Aplicades, Universitat de Vic, Sagrada Família 7, 08500–Vic, Barcelona, Spain
E-mail: montserrat.corbera@uvic.es

JAUME LLIBRE

Departament de Matemàtiques, Universitat Autònoma de Barcelona, 08193 – Bellaterra, Barcelona, Spain
E–mail: jllibre@mat.uab.es

We consider the circular Sitnikov problem as a special case of the restricted spatial isosceles 3–body problem. In appropriate coordinates we show the existence of 2–dimensional invariant tori that are formed by union of either periodic or quasiperiodic orbits of the circular Sitnikov problem, these tori are not KAM tori. We prove that such invariant tori persist when we consider the spatial isosceles 3–body problem for sufficiently small values of one of the masses. The main tool for proving these results is the analytic continuation method of periodic orbits.

1 Introduction

The main objective of this work is to prove the existence of 2–dimensional invariant tori filled of periodic or quasiperiodic orbits for the spatial isosceles 3–body problem. We note that in particular these tori are 2–dimensional invariant tori for the general spatial 3–body problem. We start reducing, with the help of appropriate coordinates, the dimension of the phase space of the isosceles problem, obtaining in this way the reduced isosceles problem. We see (in Theorem 2) that our tori filled of periodic or quasiperiodic orbits come from periodic orbits of the reduced isosceles problem. Using the analytic continuation method, we prove (in Theorem 6) the existence of symmetric periodic orbits of the reduced isosceles problem, for sufficiently small values of one of the masses, near the known periodic orbits of the reduced circular Sitnikov problem (a particular reduced restricted isosceles problem). Finally we analyze the 2–dimensional invariant tori of the isosceles problem that come from those periodic orbits.

In this paper we present results without proofs. The proofs can be found in Corbera and Llibre[2], and they constitute the main results of the Ph. D. of the first author.